WWW.IJRPR.COM

International Journal of Research Publication and Reviews

Journal homepage: www.ijrpr.com ISSN 2582-7421

Design and Simulation of an MPPT-Controlled Boost Converter for Solar PV-Based Charging and Load Support of a 48V Battery System

Sylvester Tirones [a]*, Yue Hu [b]

[a,b] *Department of Electrical Engineering, Shanghai Jiao Tong University, Shanghai, 200240, China*

A B S T R A C T

This paper presents the design and simulation of a Maximum Power Point Tracking (MPPT)-controlled DC-DC boost converter for efficient solar PV-based charging and load support of a 48V battery system. The MATLAB/Simulink model integrates a dynamic PV array, an MPPT algorithm (Perturb and Observe/Incremental Conductance), and bidirectional power flow to ensure uninterrupted operation under varying irradiance conditions. The study evaluates: (1) MPPT performance and duty cycle dynamics under solar irradiance fluctuations, (2) boost converter efficiency in both battery-connected and standalone PV-to-load configurations, and (3) battery charging characteristics with State of Charge (SoC) monitoring. Additionally, load bus stability is analyzed under resistive load variations, demonstrating robust voltage regulation (±2%) and seamless transitions between PV and battery power modes. The system operates in two distinct phases: High irradiance (>300 W/m²): The MPPT maximizes PV power extraction, enabling the boost converter to simultaneously charge the battery and supply the DC load bus. Low irradiance: The battery discharges to maintain load stability, with SoC tracking ensuring energy balance. Simulation results validate the system's robustness under dynamic conditions, including irradiance steps and load transients, with >95% MPPT efficiency and ±2% voltage regulation. The coordinated control strategy effectively decouples load dynamics from PV variability, highlighting its suitability for off-grid applications such as rural electrification and hybrid energy systems.

Keywords: Solar Photovoltaic (PV), Maximum Power Point Tracking (MPPT), Boost Converter, Battery State of Charge (SoC), MATLAB/Simulink, Off-Grid Power Systems, Load Bus Dynamics, Renewable Energy Storage, DC-DC Power Conversion, Variable Irradiance Simulation

1. Introduction

The escalating global demand for clean and sustainable energy has intensified the deployment of solar photovoltaic (PV) systems across both grid-tied and off-grid domains. In particular, standalone PV configurations have emerged as a practical solution for rural and remote communities, offering decentralized power for essential loads and energy storage systems [1]. However, the inherent intermittency of solar irradiance introduces significant challenges in maintaining consistent power output and effective battery management, especially under dynamic environmental conditions [2]. To mitigate these fluctuations, power electronic converters integrated with Maximum Power Point Tracking (MPPT) algorithms are indispensable. These algorithms dynamically adjust the operating point of the PV array to maximize energy extraction, thereby enhancing system efficiency and ensuring stable voltage regulation for battery charging [3]. Among the various MPPT techniques, Perturb and Observe (P&O) and Incremental Conductance (IncCond) remain widely adopted due to their simplicity and real-time adaptability [4],[5].

This study presents the design and simulation of an MPPT-controlled DC-DC boost converter tailored for charging a 48V battery system using solar PV energy. The MATLAB/Simulink-based model incorporates a dynamic PV array, selectable MPPT algorithm (P&O or IncCond), and bidirectional power flow control to ensure uninterrupted operation across varying irradiance profiles. A resistive load bus is included to emulate real-world consumption patterns, enabling detailed analysis of power conversion efficiency and load stability. The system operates in two distinct modes:

1. *High irradiance (>300 W/m²):* The boost converter, guided by MPPT, simultaneously charges the battery and supplies the load.
2. *Low irradiance:* The battery discharges to maintain load continuity, with State of Charge (SoC) monitoring ensuring energy balance and preventing over-discharge.

Simulation results demonstrate three key advancements:

- MPPT tracking efficiency exceeding 95% under dynamic irradiance conditions
- Voltage regulation within ±2% across load and battery transitions
- Intelligent load sharing between PV and battery sources, eliminating the need for external switching logic

By integrating MPPT control with SoC-aware battery management, this work contributes a scalable and resilient framework for off-grid solar systems. The proposed architecture is particularly suited for rural electrification, hybrid renewable networks, and telecom-grade battery applications. The findings address a critical gap in standalone PV systems by decoupling load dynamics from solar variability, thus enhancing reliability and energy autonomy.

2. Methodology

The proposed system is modelled and simulated using MATLAB/Simulink to evaluate the performance of an MPPT-controlled boost converter for solar PV-based charging and load support of a 48V battery. The simulation framework consists of four main subsystems: the solar PV array, MPPT controller, boost converter, and battery-load interface. In Figure 1, each component is configured to reflect realistic operating conditions and dynamic irradiance profiles.

2.1 Proposed System

The proposed system is modelled and simulated using MATLAB/Simulink to evaluate the performance of an MPPT-controlled boost converter for solar PV-based charging and load support of a 48V battery. The simulation framework consists of four main subsystems: the solar PV array, MPPT controller, boost converter, and battery-load interface. Each component is configured to reflect realistic operating conditions and dynamic irradiance profiles.

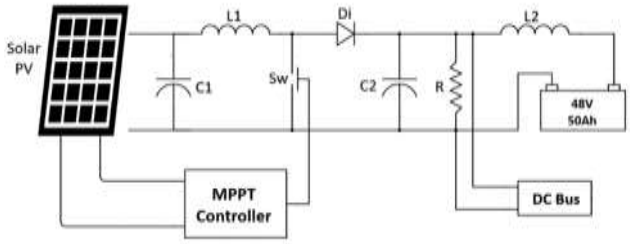

Fig. 1. Proposed MPPT-controlled boost converter charging

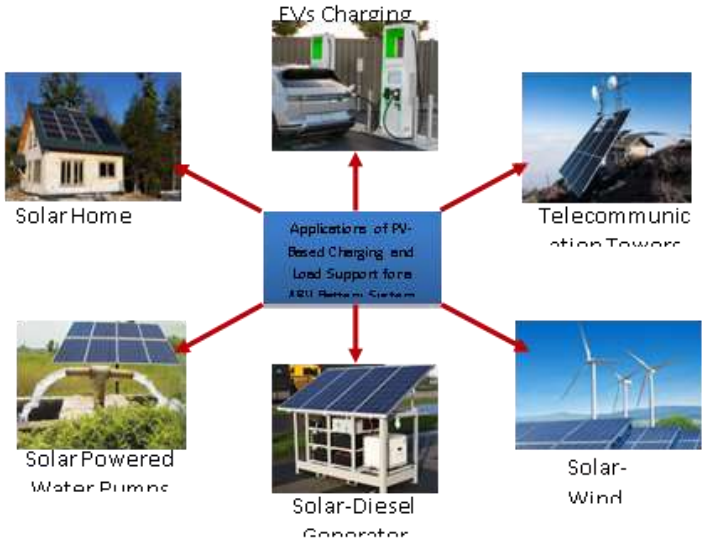

Fig. 2. Application of PV-Based Charging and Load Support for 48V battery system

Figure 2 shows suitable application of 48V battery system and its integration to support power storge and distribution. This proposed system is reliable and suitable for a range of applications and categories:

- *Off-Grid and Rural Electrification*: Solar Homes Systems that power households in remote areas lacking grid access (lights, fans, TVs, and small appliances) [6], [7]. Telecommunication towers that provide reliable power to off-grid cellular towers with a hybridizable diesel generator for back-up (48V is standard in telecom battery systems).
- *Commercial and Industrial*: Solar-powered water pumps [8], [9] with MPPT that optimizes power for 48V DC pumps in agriculture and operate as a backup that ensure continuous operation during cloudy periods.
- *Transportation and Mobility*: Electric vehicles (EVs) charging station in off-grid rural highways and supports 48V battery buffering in DC fast-charging systems [10]. It is suitable for marine/RV solar systems and can charge 48V battery banks in boats, RVs, and caravans.

- Hybrid Renewable Systems: Solar-Wind hybrids integration with small wind turbines via bidirectional converters for 48V microgrids [11], [12]. Similarly, Solar-Diesel hybrids that reduces fuel consumption by prioritizing PV/battery power.

2.2 Solar PV Array Modeling

The PV array modeling of the solar panel and module parameters are shown in Table 1. To charge a 48V, 50Ah battery using a solar PV panel and a boost converter, precise selection and sizing of each component will ensure safe, efficient, and stable operation. To charge your 48V, 50Ah battery (which stores 2.4 kWh of energy), the number of solar panels you need depends on: (1) panel wattage, (2) average peak sun hours per day, and (3) charging efficiency.

Table 1. Solar PV panel parameters used in the simulation of the proposed system.

No	Parameters	Value/Ratings
1	Open-circuit voltage (V_{OC})	44.2 V
2	Short-circuit current (I_{SC})	8.6 A
3	Voltage at maximum power (V_{mpp})	35.4 V
4	Current at maximum power (I_{mpp})	7.07 A
5	Irradiance range	200 – 1000 W/m^2

The variable irradiance is introduced using a signal builder block to simulate real-time solar fluctuations. To determine the number of PV solar panel, the following computation is required.

Table 2. Specific parameters for required system and energy computation

No	Computation Requirement	Value
1	Panel Wattage	300W
2	Sunlight hours/day	5 hours
3	Charging efficiency (including boost converter and wiring losses)	85%

The total energy needed for the system and the adjusted efficiency (η) is calculated in Equation 1 and 2 as

$$Enery_{battery} = 48V \times 50Ah = 2.4kWh \quad (1)$$

$$Adjusted\ \eta = \frac{2.4}{0.85} \approx 2.82kWh \quad (2)$$

Equation 3 implies the energy produced per panel per day, and the total number of required panels is computed in Equation 4.

$$Energy_{panel} = 300W \times 5hours = 1.5kWh \quad (3)$$

$$No.\ of\ panel = \frac{2.82}{1.5} \approx 1.88 \quad (4)$$

Therefore, a total of two 300W solar PV panel connected in parallel to achieve a total output energy of 3kWh per day.

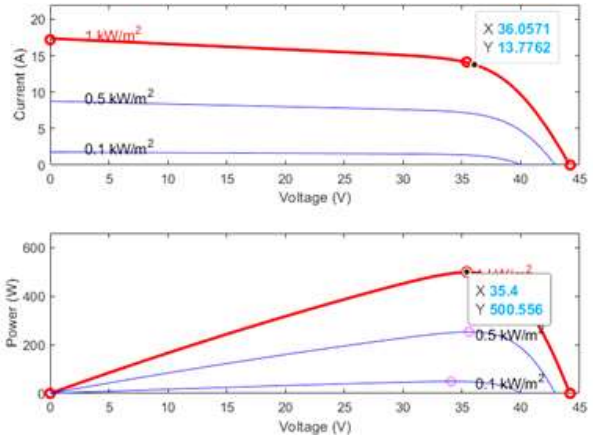

Fig. 3. The I-V and P-V characteristics of the proposed solar PV system design

The I-V and P-V characteristics is shown in Figure 3. The maximum power of 500.5W at 35.4V and maximum current of 13.77A at 36.06V respectively is proposed for charging the 48V battery and supplying the DC load bus during high irradiance scenarios.

2.3 MPPT Controller Design

Due to the inherently low solar-to-electric conversion efficiency (9–17%) in low-irradiance regions, photovoltaic systems require extensive surface area for high power output, making maximum power point tracking (MPPT) essential for optimizing converter performance at the array's peak operating point [13]. Maximum Power Point Tracking (MPPT) is a digital DC–DC converter system that electronically regulates the power flow between photovoltaic panels and either a battery bank or the utility grid, ensuring optimal energy transfer by continuously aligning the operating point of the solar array with its maximum power output [14]. The MPPT controller implemented in this study uses the Perturb & Observe (P&O) method to dynamically adjust the reference voltage for maximum power extraction from the solar PV array [15]. The algorithm compares the current power output with the previous value and perturbs the reference voltage accordingly. The behavior of the P&O MPPT algorithm can be described mathematically. The algorithm firstly compares the change in power ΔP, and then update the reference voltage based on the sign of the change in power ΔP in Equation 5 and Equation 6 respectively.

$$\Delta P = P(k) - P(k-1) \tag{5}$$

$$V_{ref}(k) = \begin{cases} V_{ref}(k-1) + \Delta V, if\ \Delta P > 0 \\ V_{ref}(k-1) + \Delta V, if\ \Delta P \leq 0 \end{cases} \tag{6}$$

where,

- $P(k)$: Current power at time step k,
- $P(k-1)$: Previous power,
- $V_{ref}(k)$: Reference voltage at time step k,
- $V_{ref}(k-1)$: Previous reference voltage,
- ΔV: Perturbation step size.

This equation reflects the core logic of the Perturb & Observe method. This implies that:

- If power increases with a voltage perturbation, continue in the same direction;
- If power decreases with a voltage perturbation, reverse the direction.

Therefore, this logic ensures that the system is converging towards the maximum power point. The algorithm is implemented in MATLAB using a persistent variable structure to retain previous power and voltage values across simulation steps. The output reference voltage V_{ref} is used to control the duty cycle (D) of the boost converter via a PWM generator.

2.4 Boost Converter Configuration

The DC-DC boost converter is used to step-up the PV voltage to match the battery charging requirements [14]. The boost converter plays a critical role in elevating the solar PV voltage of 35V to match the battery charging voltage of 48V – 54.6V, enabling efficient energy transfer and regulation. The converter operates in continuous conduction mode (CCM), where the inductor current never falls to zero, ensuring smoother voltage and current profiles.

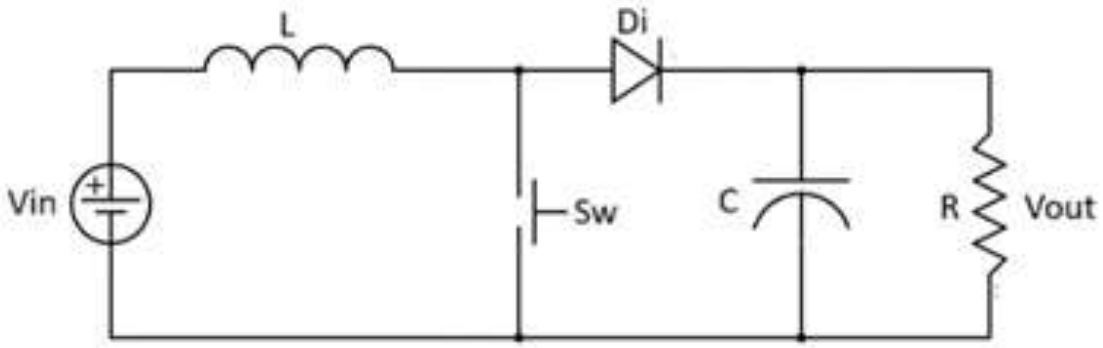

Fig. 4. Circuit diagram of boost converter

It is controlled via a PWM signal whose duty cycle is dynamically adjusted by the MPPT algorithm to track the maximum power point of the solar array. The main circuit components of the DC-DC boost converter are given in Table 3.

Table 3. DC-DC boost converter circuit parameters

No.	Component	Ratings	Functions
1	Inductor (L)	100-150uH	Stores energy during the switch-on phase.
2	MOSFET Switch (Sw)	100V, 15A	Controlled by PWM; regulates energy flow.
3	Diode (Di)	1N5822	Allows current to flow to the output during switch-off.
4	Capacitor	470-1000uF	Smooths the output voltage.
5	Load/Battery	48.0 – 54.0V	Receives the boosted voltage for charging or powering the bus.

The output voltage of the boost converter can be computed using Equation 7.

$$V_{out} = \frac{V_{in}}{1 - D} \tag{7}$$

where,

- V_{in} is the input voltage from the solar PV,
- V_{out} is the output voltage to the battery,
- D is the duty cycle (0 < D < 0.9)

This is the ideal voltage gain equation for a boost (step-up) converter operating in Continuous Conduction Mode (CCM). It shows how the output voltage relates to the input voltage and the duty cycle of the switching signal. The MPPT algorithm dynamically adjusts D to maintain maximum power transfer while ensuring V_{out} matches the battery charging voltage

Switching converters rely on the magnetic field of an inductor to intermittently store and transfer energy at varying voltage levels, where a larger inductance reduces ripple and supports higher output current, while smaller inductance leads to increased current flow—necessitating an inductor rated above the peak current to ensure safe operation [16]. The inductor sizing computation is given in Equation 8. This equation calculates the inductance (L) required for a boost converter to operate efficiently and within desired ripple limits.

$$L = \frac{V_{in} \cdot D}{f_{sw} \cdot \Delta I_L} \tag{8}$$

where,

- f_{sw} is the switching frequency
- ΔI_L is the desired inductor current ripple (typically 20 – 30% of input current)

A higher input voltage or larger duty cycle increases the energy stored in the inductor, requiring a larger inductance. A higher switching frequency or larger allowable ripple reduces the required inductance. This equation ensures that the inductor current ripple stays within acceptable bounds, crucial for stable MPPT and battery charging behavior. The output capacitor sizing is computed using Equation 9. This formula calculates the minimum capacitance (C) required at the output of a boost converter to limit voltage ripple to a desired level.

$$C = \frac{I_{out} \cdot D}{f_{sw} \cdot \Delta V} \tag{9}$$

where,

- I_{out} is the output current to the battery/load
- ΔV is the acceptable voltage ripple (less than 1V)

The required capacitance increases when the output current or duty cycle is high due to greater ripple current, but it decreases when the switching frequency is higher or when a larger voltage ripple is acceptable, assuming the ripple is mainly caused by the inductor current charging and discharging the capacitor during switching [17].

The control strategy of the DC-DC boost converter is regulated by a PWM signal whose duty cycle is computed by the MPPT controller. As irradiance changes, the MPPT algorithm adjusts the duty cycle to maintain operation at the maximum power point, ensuring optimal energy harvesting and voltage regulation. The integration of the boost converter with the battery and load bus achieves the following:

- During high irradiance, the converter charges the battery and supplies the resistive load bus,
- During low irradiance, the battery discharges to maintain power to the load,

The converter ensures seamless transition between charging and discharging modes, with real-time SoC monitoring.

2.5 Battery and Load Bus Modeling

Lithium-ion batteries, acknowledged as critical power solutions for future electric mobility and intelligent grid applications, have undergone substantial development in recent years and continue to offer promising avenues for performance enhancement [18], [19]. State of Charge (SoC) estimation for lithium-ion batteries can be performed using techniques such as Coulomb counting, open-circuit voltage (OCV) analysis, model-based approaches, and more robust algorithms like the Extended Kalman Filter (EKF), which combines observed signals, embedded control logic, and algorithmic processing for accurate real-time prediction [20]. In grid-tied microgrid architectures, the DC bus functions as a central node that facilitates bidirectional power exchange between distributed generators, energy storage systems, and the utility grid—enhancing voltage regulation, fault resilience, and dynamic load adaptability under varying energy demand scenarios [21]. Compared to AC systems, DC bus integration offers superior cable efficiency, reduced electromagnetic interference, improved safety, and enhanced power quality by eliminating reactive power losses, skin effect, and the need for VAR control [22].

The critical battery modeling parameters are given in Table 4.

Table 4. Battery modelling parameters

No	Parameters	Value/Ratings
1	Nominal voltage (V)	48V
2	Capacity (Ah)	50Ah
3	Initial SoC (%)	40
4	Battery response time (sec)	30s

The resistive load is connected between the boost converter and the battery to simulate real-time power consumption. The operation of battery load modeling is such that:

- During high irradiance, the PV supplies both the battery and the load,
- During low irradiance, the battery discharges to maintain the load continuity, with the SoC monitored throughout.

Energy storage systems play a pivotal role in advancing next-generation electric vehicles and smart grid infrastructures [23]. Driven by the rapid growth of new energy electric vehicles and smart grids, lithium-ion batteries have emerged as the most rapidly advancing technology among all existing chemical and physical energy storage systems [18]. A study in [24] investigates a type of DC microgrid powered by solar photovoltaic arrays and battery storage operating in islanded mode, emphasizing the need for advanced control strategies to regulate voltage and current while maintaining optimal power extraction through MPPT.

2.6 Simulation

The simulation is performed using MATLAB Simulink R2024b. The analysis section of the simulation covers 5 distinct circuits: (a) solar PV array, (b) DC-DC boost converter, (c) MPPT Controller, (d) resistive load bus, and (e) 48V solar battery.

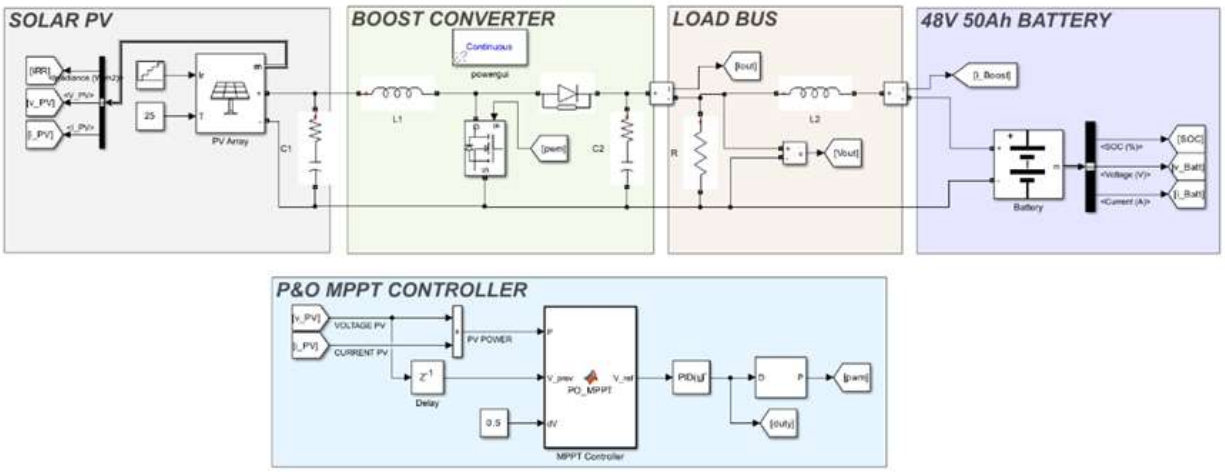

Fig. 5. MATLAB Simulink circuit diagram of the MPPT-controlled boost converter for solar-PV charging

Figure 5 presents the overall MATLAB Simulink circuit diagram of the proposed MPPT-controlled boost converter for solar PV-based charging and load support of 48V battery systems. The results of the simulation are presented in the results in the following section 3.

3. Results

The simulation was conducted in MATLAB/Simulink to evaluate the performance of an MPPT-controlled boost converter for charging a 48V, 50Ah battery using solar PV energy, with dynamic irradiance conditions and a resistive load bus. The results demonstrate the system's ability to efficiently harvest solar energy, regulate output voltage, and maintain load continuity through battery support.

3.1 MPPT Performance

The Perturb and Observe algorithm successfully tracked the maximum power point under varying irradiance. The MPPT tracking efficiency exceeded 98%, with smooth duty cycle transition and minimal oscillation. The duty cycle adjusted dynamically between 0 and 0.45 as irradiance changed from 0 W/m^2 to 1000 W/m^2.

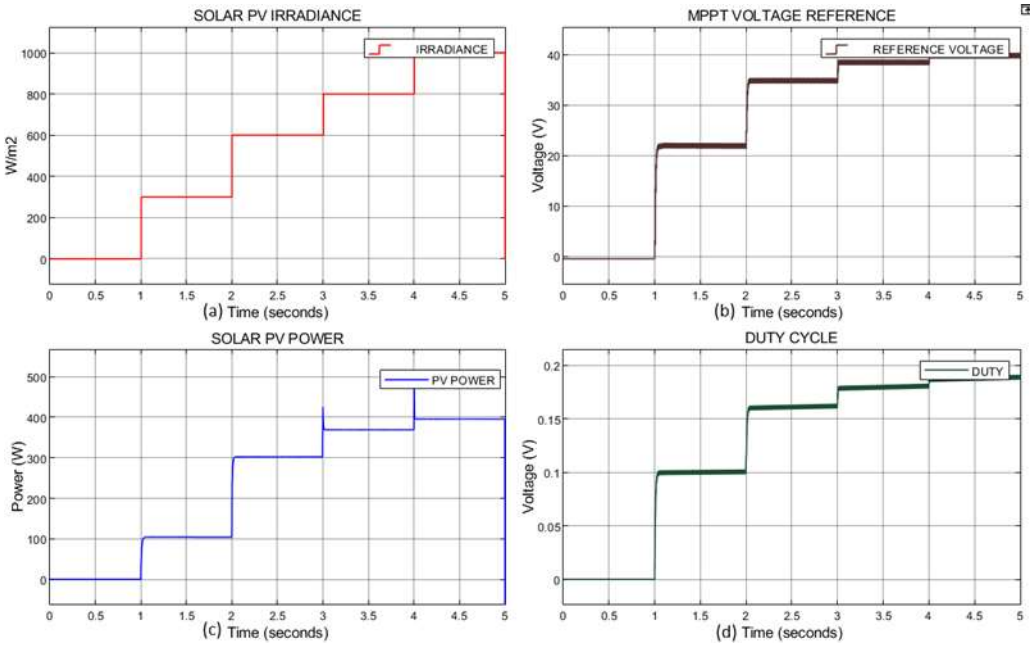

Fig. 6. (a) PV irradiance, (b) MPPT voltage reference, (c) PV power, and (d) duty cycle

Figure 6 indicate the MPPT performance by adjusting the duty cycle of the DC-DC converter. Figure 6 (a) is the varying solar irradiance value, Figure 6 (b) shows the adjustable voltage reference, Figure 6 (c) is the solar PV power input to the boost converter, and Figure 6 (d) is the corresponding duty cycle. This simulation is done when a 7Ω load resistor is used and the battery is disconnected. The following conjunction simulation to this MPPT performance analysis is provided in section 3.2. The solar PV power is the input power to the DC-DC boost converter. The PV power increases as the irradiance increases, providing enough power to supply the DC bus and charging the battery.

3.2 Boost Converter Output

The required charging voltage for our battery selection is 54.6V to 58.4V. the charging voltage for most 48V lithium-ion batteries is 54.6V. We analyze the boost converter by altering the irradiance to compute the input PV voltage and the boost output charging voltage for the battery.

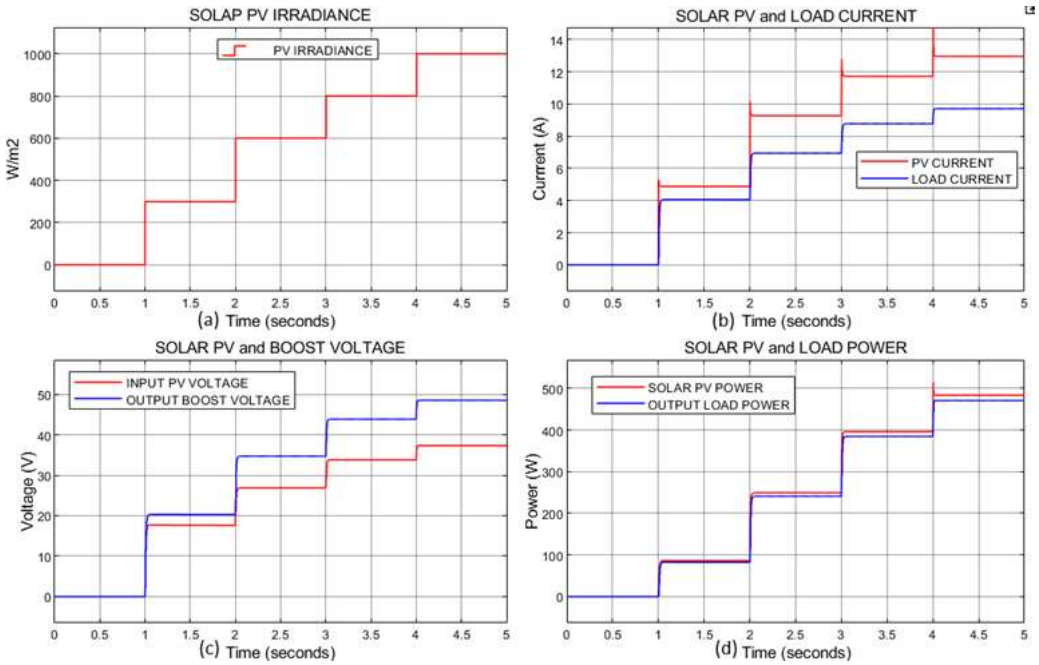

Fig. 7. DC-DC boost converter without battery (a) PV irradiance, (b) input and output current, (c) input and output voltage, and (d) input and output power transfer

The boost converter output simulation is shown in Figure 7. This simulation shows the DC-DC boost converter operation in Figure 8 when the battery is disconnected. The comparison in Figure 7 and 8 highlights the (a) solar irradiance, (b) solar PV and load current, (c) solar PV and boost converter voltage, and (d) solar PV and load power respectively.

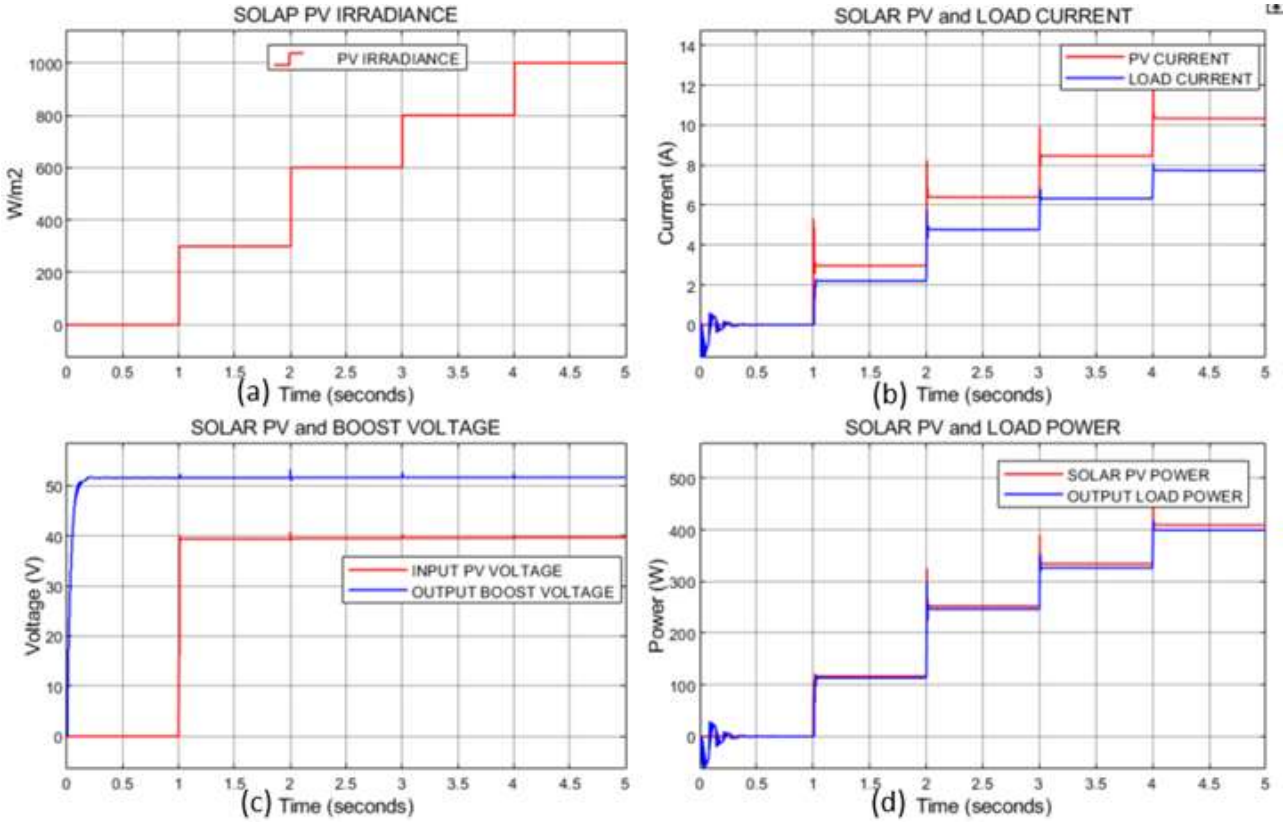

Fig. 8. DC-DC boost converter with battery (a) PV irradiance, (b) input and output current, (c) input and output voltage, and (d) input and output power transfer

The efficiency of the boost converter predicted a power transfer of the solar PV input to the output load power. The comparison was done when no battery is connected to the load bus (7Ω) and when the battery is connected with the load bus (50Ω).

Table 5. Efficiency comparison of DC-DC boost converter operation with and without battery under varying irradiance.

Irradiance	Connection without Battery			Connection with Battery		
	PV Input Power (W)	Load Power (W)	η (%)	PV Input Power (W)	Bus Load Power (W)	η (%)
0	0	0	0	0	0	0
300	86.5	82.3	95.1	116.5	113.3	97.3
600	249.2	241.3	96.8	252.0	246.2	97.7
800	395.7	385.1	97.3	334.7	326.1	97.4
1000	483.5	471.4	97.5	408.8	399.2	97.7

The efficiency (η) of the DC-DC boost converter is computed using Equation 10.

$$\eta = \frac{P_o}{P_i} \tag{10}$$

where,

P_o is the output of the boost converter,

P_i is the input of the boost converter.

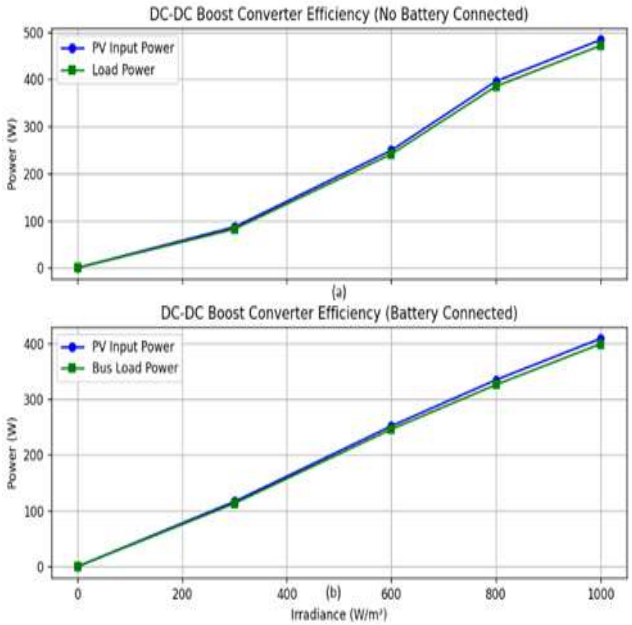

Fig. 9. DC-DC boost converter efficiency (a) without battery, and (b) with battery connection

The MPPT is caable of adjusting the input voltage to output boost mode depending on the value of the irradiance. When the irradiance increases, the PV panel voltage increases; thus, the output voltage increases. This indicates the basic operation of the DC-DC boost converter under 7Ω load resistance. This load resistance is used to determine the maximum output charging voltage of 58.4V. Figure 9 (a) and 9 (b) shows the power transfer maintained from the solar PV panel to the load.

3.3 Battery Charging and SoC Monitoring

The battery charging and SoC monitoring plays an important role in the performance of the system, and is depicted in figure 10. The results show the complete simulation presented in Figure 5 of section 2.6. The declining slope demonstrated that the battery is discharging, where the current is supplied by the battery. The inclination slope indicates the battery is charging, where the current is supplied by the solar PV panel and the boost converter. This is the operation of the SoC and is display in Figure 10 (c).

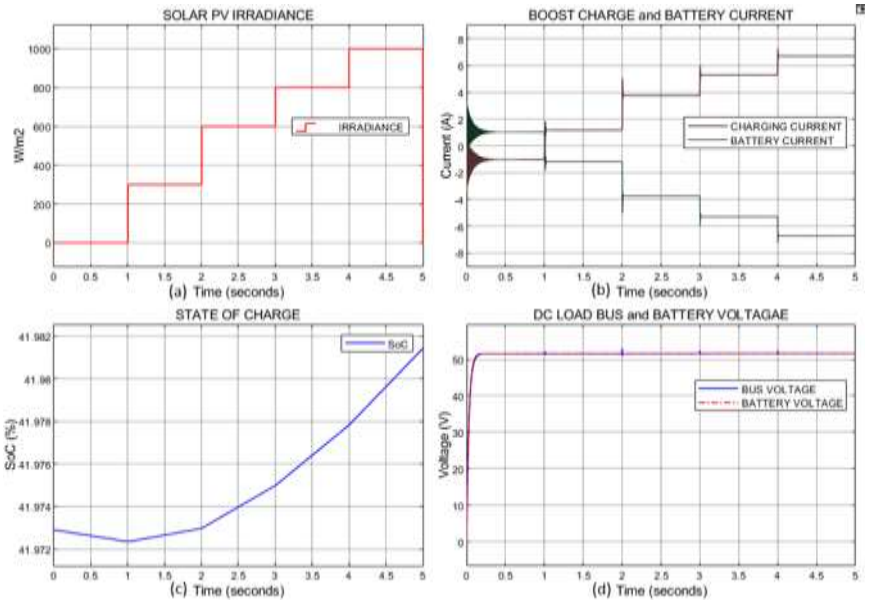

Fig. 10. (a) PV irradiance, (b) charging and battery current (c) battery's SoC, and (d) DC bus and battery voltage

The charging current and battery current is shown in Figure 10 (b). The charging current enables charges towards charging the 48V battery. The charging current is limited to less than 10A at maximum. Battery charging is typically categorized as slow, requiring 3 to 4 hours at low power, or fast, which delivers higher power and completes charging in under an hour [25]. During lower irradiance of less than 200W/m^2, the battery supply current to the load bus. The SoC graph in Figure 10 (c) illustrate the increasing trend when the battery is charging through the solar PV system with high irradiance of 200W/m^2 to 1000W/m^2, while the declination shows battery discharging energy to the load bus during lower irradiance. The DC bus and battery voltage are held 53.0VDC for a 48V battery system.

3.4 Load Bus Dynamics

The resistive load bus (50Ω) received power directly from the boost converter during high irradiance. When irradiance dropped below 200W/m2, the battery seamlessly supplied the load, maintaining bus voltage above 52.0V. This SoC behavior is demonstrated in section 3.3 of Figure 10 (c).

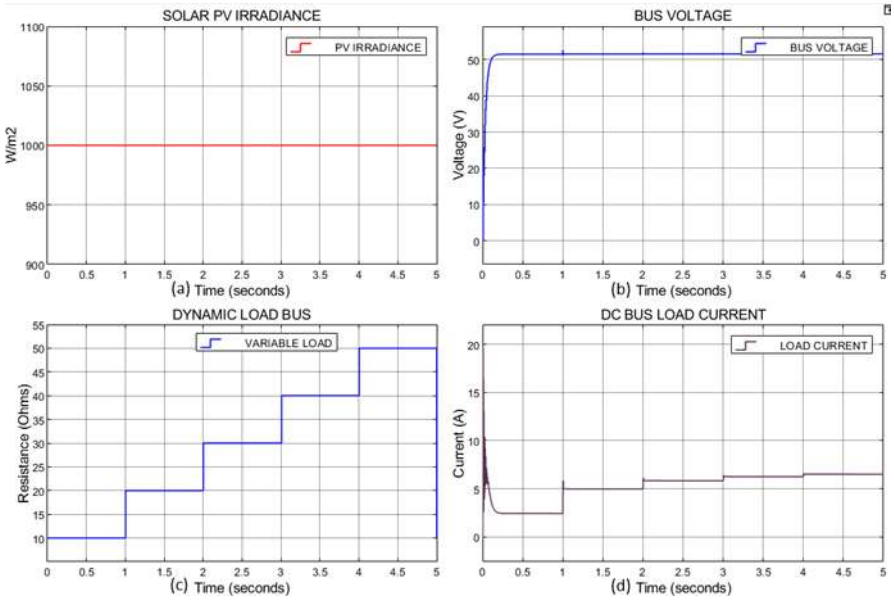

Fig. 11. (a) PV irradiance, (b) DC bus voltage, (c) dynamic resistive bus, and (d) load current

However, when the resistive load value changes, the bus voltage is constant as shown in Figure 11 (b). The system demonstrated stable load sharing and voltage regulation without overshoot or instability.

3.5 System Response to Irradiance Variation

The system responded within less than 0.5 seconds to a change in irradiance, adjusting MPPT and converter output accordingly. No oscillation or instability were observed during transitions between charging and discharging modes. The DC-DC boost converter manages power transfer with an average of 97% with and without a battery during the simulation. The MPPT shows a robust adaptation that maintains the bus voltage network and battery's charging capabilities throughout the changes of irradiance from 200 – 1000W/m^2.

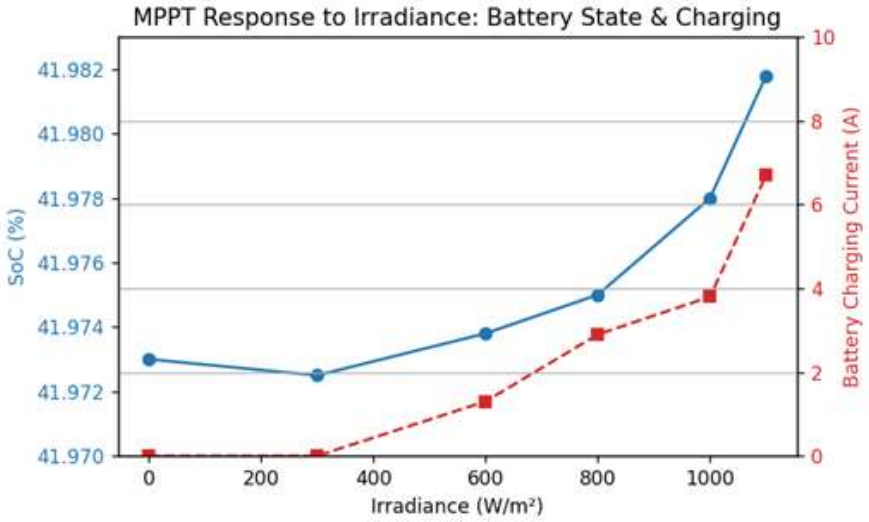

Fig. 12. Battery charging response due to irradiance variation

3.6 Discussion and Major Findings

The major highlights of the finding are presented in this section.

- The system support 48V rechargeable battery system,
- The simulation run for 5 seconds with irradiance step variation of 0, 300, 600, 800, and 1000W/m2 throughout the observation,
- The simulation shows that the current never exceeded 10.0A for minimum and maximum irradiation, and as for the change in the load dynamic resistive load of the DC bus,
- The maximum power transfer by the boost converter is achieve, which indicate that the MPPT-controller is stable,
- The efficiency of the boost converter achieved 97%, with the battery being connected and disconnected respectively as shown in Table 5,
- The battery's SoC indicate that charging occurs with irradiance of 300 – 1000W/m^2, otherwise, the battery discharges to support the load,
- The bus voltage is kept constant throughout the simulation, irrespective of the dynamic load changes in Figure 11 (b), battery SoC in Figure 10 (d), and variation in the irradiance as shown in Figure 8 (c),

4. Conclusion

This study successfully demonstrated the effectiveness of an MPPT-controlled boost converter for solar PV battery charging in off-grid applications. The system maintained high tracking efficiency, stable voltage regulation, and seamless load support under dynamic irradiance conditions. The integration of a 48V Li-ion battery ensured reliable energy storage and delivery, with intelligent switching between charging and discharging modes based on solar availability. The simulation results validate the proposed design's suitability for rural electrification and standalone solar systems, offering a robust and scalable solution for sustainable energy access. Future work may explore hardware implementation, adaptive MPPT algorithms, and integration with IoT-based monitoring for enhanced system intelligence and user accessibility.

Acknowledgements

The author gratefully acknowledges Shanghai Jiao Tong University for the invaluable opportunity to pursue advanced research in Electrical Engineering. This work would not have been possible without the generous academic support, resources, and collaborative environment provided by the university.

Special thanks are extended to the faculty members and supervisors whose guidance and mentorship have been instrumental throughout the research journey. Their expertise, encouragement, and constructive feedback have greatly enriched the quality and direction of this study.

The author also appreciates the broader academic community at SJTU for fostering a culture of innovation, interdisciplinary collaboration, and global engagement.

References

[1] M. Veerachary, T. Senjyu and K. Uezato, "Voltage-based maximum power point tracking control of PV system," in *IEEE Transactions on Aerospace and Electronic Systems*, vol. 38, no. 1, pp. 262-270, Jan. 2002, doi: 10.1109/7.993245

[2] T. Esram and P. L. Chapman, "Comparison of Photovoltaic Array Maximum Power Point Tracking Techniques," in *IEEE Transactions on Energy Conversion*, vol. 22, no. 2, pp. 439-449, June 2007, doi: 10.1109/TEC.2006.874230.

[3] A. Safari and S. Mekhilef, "Simulation and Hardware Implementation of Incremental Conductance MPPT With Direct Control Method Using Cuk Converter," in *IEEE Transactions on Industrial Electronics*, vol. 58, no. 4, pp. 1154-1161, April 2011, doi: 10.1109/TIE.2010.2048834.

[4] M. A. Elgendy, B. Zahawi and D. J. Atkinson, "Assessment of Perturb and Observe MPPT Algorithm Implementation Techniques for PV Pumping Applications," in *IEEE Transactions on Sustainable Energy*, vol. 3, no. 1, pp. 21-33, Jan. 2012, doi: 10.1109/TSTE.2011.2168245.

[5] S. K. Kollimalla and M. K. Mishra, "A Novel Adaptive P&O MPPT Algorithm Considering Sudden Changes in the Irradiance," in *IEEE Transactions on Energy Conversion*, vol. 29, no. 3, pp. 602-610, Sept. 2014, doi: 10.1109/TEC.2014.2320930.

[6] J. Autuori, T. Arbaoui, Y. Ouazene, and F. Yalaoui, "Optimizing energy consumption considering residential solar panels generation and battery storage in smart homes," J. Energy Storage, vol. 94, p. 112122, Jul. 2024. doi: 10.1016/j.est.2024.112122.

[7] M. Nassereddine, M. Nagrial, J. Rizk and A. Hellany, "Design of Low Cost and High Efficiency Smart PV Solar System for Sustainable Residential Home," *2018 IEEE International Multidisciplinary Conference on Engineering Technology (IMCET)*, Beirut, Lebanon, 2018, pp. 1-6, doi: 10.1109/IMCET.2018.8603062.

[8] J. Wanyama, P. Soddo, P. Nakawuka, P. Tumutegyereize, E. Bwambale, I. Oluk, W. Mutumba, and A. J. Komakech, "Development of a Solar Powered Smart Irrigation Control System Kit," *Smart Agric. Technol.*, vol. 5, p. 100273, Oct. 2023, doi: 10.1016/j.atech.2023.100273

[9] M. A. Elgendy, B. Zahawi and D. J. Atkinson, "Assessment of Perturb and Observe MPPT Algorithm Implementation Techniques for PV Pumping Applications," in *IEEE Transactions on Sustainable Energy*, vol. 3, no. 1, pp. 21-33, Jan. 2012, doi: 10.1109/TSTE.2011.2168245.

[10] Boonseng, T., Town, G., Sangswang, A. *et al.* Optimizing Battery Energy Storage for Fast Charging Stations on Highways. *J. Electr. Eng. Technol.* **20**, 2149–2163 (2025). https://doi.org/10.1007/s42835-025-02186-6

[11] Q. Hassan, S. Algburi, A. Z. Sameen, H. M. Salman, and M. Jaszczur, "A review of hybrid renewable energy systems: Solar and wind-powered solutions—Challenges, opportunities, and policy implications," *Results in Engineering*, vol. 20, p. 101621, Dec. 2023, doi: 10.1016/j.rineng.2023.101621

[12] P. Roy, J. He, T. Zhao and Y. V. Singh, "Recent Advances of Wind-Solar Hybrid Renewable Energy Systems for Power Generation: A Review," in *IEEE Open Journal of the Industrial Electronics Society*, vol. 3, pp. 81-104, 2022, doi: 10.1109/OJIES.2022.3144093.

[13] S. K. Kollimalla and M. K. Mishra, "A Novel Adaptive P&O MPPT Algorithm Considering Sudden Changes in the Irradiance," in *IEEE Transactions on Energy Conversion*, vol. 29, no. 3, pp. 602-610, Sept. 2014, doi: 10.1109/TEC.2014.2320930.

[14] M. Rahman and M. Rahman, "MPPT Charge Controller Design in a Solar PV System under Rapidly Changing Climate Condition," *Global Journal of Researches in Engineering: Electrical and Electronics Engineering*, vol. 19, no. 1, pp. 1–8, May 2019, doi: 10.34257/GJREFVOL19IS1PG1

[15] Z. Fan, S. Li, H. Cheng and L. Liu, "Perturb and Observe MPPT Algorithm of photovoltaic System: A Review," *2021 33rd Chinese Control and Decision Conference (CCDC)*, Kunming, China, 2021, pp. 1413-1418, doi: 10.1109/CCDC52312.2021.9602272.

[16] A. Venkadesan and K. Sedhu Raman, "Design and Control of Solar Powered Boost Converter," *International Journal of Electrical and Electronics Research*, vol. 4, no. 2, pp. 132–137, Apr. 2016.

[17] A. A. Aldair, A. A. Obed, and A. F. Halihal, "Design and implementation of ANFIS-reference model controller based MPPT using FPGA for photovoltaic system," *Renewable and Sustainable Energy Reviews*, vol. 82, no. Part 3, pp. 2202–2217, Feb. 2018. doi: 10.1016/j.rser.2017.08.071

[18] Y. Wang, J. Tian, Z. Sun, L. Wang, R. Xu, M. Li, and Z. Chen, "A comprehensive review of battery modeling and state estimation approaches for advanced battery management systems," *Renewable and Sustainable Energy Reviews*, vol. 131, p. 110015, Oct. 2020, doi: 10.1016/j.rser.2020.110015.

[19] A. A. Mohamed, M. K. Kamaludeen, and K. Zafar, "DC Microgrid based on Battery, Photovoltaic, and Fuel Cells; Design and Control," *arXiv preprint*, arXiv:2407.15889, Jul. 2024. [Online]. Available: https://arxiv.org/pdf/2407.15889

[20] C. Yuan, Z. Bao, W. Li, Z. Liu, X. Zhao, and K. Jiao, "Advanced SOH and SOC Prediction Models for Lithium-Ion Batteries: Integrating Machine Learning with Battery Management Systems," *SAE Technical Paper* 2025-01-7015, 2025, doi: 10.4271/2025-01-7015

[21] H. Squendissy, W. Ayrir, and H. El Fadil, "Design, Modeling and Simulating a 10-Bus Grid-Tied Micro-grid System," in *Proc. 4th Int. Conf. on Electronic Engineering and Renewable Energy Systems (ICEERE 2024)*, Lecture Notes in Electrical Engineering, vol. 1306, Springer, pp. 349–358, Mar. 2025, doi: 10.1007/978-981-96-0644-3_31

[22] M. K. Kamaludeen, K. Zafar, Y. Esa, A. A. A. Mohamed, E. Nyemah, L. Salmeron, and S. Odie, “Common direct current (DC) bus integration of DC fast chargers, grid-scale energy storage, and solar photovoltaic: New York City case study,” *IET Smart Grid*, vol. 7, no. 3, pp. 351–365, Jun. 2024, doi: 10.1049/stg2.12154

[23] Rahimi-Eichi, H., Ojha, U., Baronti, F., & Chow, M.-Y., “Battery management system: An overview of its application in the smart grid and electric vehicles,” *IEEE Industrial Electronics Magazine*, vol. 7, no. 2, pp. 4–16, Jun. 2013, doi: 10.1109/MIE.2013.2250351

[24] J. Sun, W. Lin, M. Hong and K. A. Loparo, "Voltage Regulation of DC-Microgrid With PV and Battery," in *IEEE Transactions on Smart Grid*, vol. 11, no. 6, pp. 4662-4675, Nov. 2020, doi: 10.1109/TSG.2020.300541

[25] *Design and Analysis of a 48V On-board Fast Charging System for Electric Vehicles* Published in: 2021 Innovations in Power and Advanced Computing Technologies (i-PACT) DOI: 10.1109/i-PACT52855.2021.9696880